

# Controlling factors in the selective conversion of *n*-butane over promoted VPO catalysts at low temperature

Nishlan Govender<sup>a</sup>, Holger B. Friedrich<sup>a,\*</sup>, Matthys Janse van Vuuren<sup>b</sup>

<sup>a</sup>*School of Pure and Applied Chemistry, University of KwaZulu-Natal, Durban 4041, South Africa*

<sup>b</sup>*Sasol Technology R&D, PO Box 1, Sasolburg 1947, South Africa*

## Abstract

Unpromoted and 1.2, 2.3 and 4.3 molar % Co:V cobalt-promoted vanadium-phosphorous-oxide (VPO) catalysts were synthesized via an organic route. The catalyst precursors were calcined and then conditioned in a reactor, forming the active vanadyl pyrophosphate (VO)<sub>2</sub>P<sub>2</sub>O<sub>7</sub> phase, which was confirmed via X-ray diffraction studies (XRD). The effect of co-promotion on the yield of maleic anhydride (MA) from *n*-butane oxidation was examined at different temperatures and gas hourly space velocities (GHSV). 2.3% Co:V was the optimum promoter loading for a high yield towards MA. Higher GHSV's proved to enhance the selectivity towards MA.

The catalysts were tested over a 200 h period, generally taking some 24 h to reach steady-state performance. The best performing catalyst yielded 45% MA at 275 °C and a GHSV of 7200 ml g<sup>-1</sup> h<sup>-1</sup>, with an *n*-butane conversion of 73%, whilst all previously reported VPO catalysts produced far lower MA yields at this temperature.

© 2004 Elsevier B.V. All rights reserved.

**Keywords:** *n*-Butane; Maleic anhydride; Cobalt; Temperature; Gas hourly space velocity; VPO catalysts

## 1. Introduction

Much research has focussed on the direct partial oxidation of alkanes to oxygenates in recent years. This is in effect the conversion of low value feedstocks to high value products. The conversion of *n*-butane to maleic anhydride (MA) has been the subject of extended research for industrial reasons due to the economic importance of MA as a chemical intermediate, and for fundamental reasons due to this reaction being very complex in that it involves a 14-electron oxidation with 8-H abstractions, 3-O insertions, and subsequent electron transfers. MA is important in a large number of chemical processes; unsaturated polyester resins being a major use amongst others, such as lube additives, paper reinforcement, agriculture and specialty chemicals. In 1995, the global production of MA had grown to an estimated 900,000 tons with a value of \$700 million [1].

This study was undertaken to investigate MA production over a vanadium phosphorous oxide (VPO) catalyst at different GHSVs, temperature and cobalt promoter loading.

The catalyst pretreatment regime and method of promoter introduction also play a significant role in the performance of the catalyst. The study was aimed at obtaining the optimum conditions for the highest yield of MA over a cobalt-promoted VPO catalyst prepared by an organic route.

Cobalt was chosen as a promoter because it was found to remarkably improve the selectivity towards MA [2]. Cobalt is also known to stabilize phosphorous in the lattice of the catalyst and reduce or prevent the sublimation of phosphorous under the high-operating temperatures around 400 °C. The excess phosphorous above the stoichiometric value could thus be maintained in the catalyst, which is required for the selective oxidation of *n*-butane [3].

## 2. Experimental

An organic-synthetic route was followed in the synthesis of the VPO catalyst. V<sub>2</sub>O<sub>5</sub> (10 g, 0.055 mol) was added to a 3:2 volumetric ratio of *iso*-butanol:benzyl alcohol solvent mixture (100 ml), which reduced the V<sub>2</sub>O<sub>5</sub>. Powdered Co(acac)<sub>3</sub> was added to the mixture before refluxing. The

\* Corresponding author.

E-mail address: [friedric@ukzn.ac.za](mailto:friedric@ukzn.ac.za) (H.B. Friedrich).

Co(acac)<sub>3</sub> amounts added during the reduction stage of the synthesis were varied for different promoter-loaded catalysts: VPO-1 (0 g); VPO-2 (0.49 g, 0.0014 mol); VPO-3 (0.97 g, 0.0027 mol) and VPO-4 (1.94 g, 0.0055 mol). The mixture was refluxed for 7 h followed by cooling overnight. *ortho*-H<sub>3</sub>PO<sub>4</sub> (11 g, 0.11 mol) was added to the cooled mixture and refluxed for a further 3 h. The mixture was cooled to yield a precipitate, which was filtered off on hardened (541) ashless filter paper. The precipitate was washed with 20 ml *iso*-butanol solvent. The precipitate was initially dried overnight in an oven set at 100 °C under an air atmosphere and then calcined under a nitrogen atmosphere at 450 °C for 5 h to yield a black catalyst referred to as the calcined catalyst. The unpromoted catalyst (VPO-1) was similarly synthesized without the addition of Co(acac)<sub>3</sub> during the reduction step.

A fixed-bed continuous flow micro-reactor with an on-line gas chromatograph (GC) was employed to test the catalysts. 1% butane in air premix was used as the feedgas. The feed lines were copper, whilst the product lines were stainless steel as the MA product is corrosive. Since the MA product is a solid at room temperature, the product lines were heated to 160 °C to prevent product condensation. The feedstream flowrate was controlled via flowmeters. The product stream was sent to two on-line 500 µL sample loops. One loop sampled to a thermal conductivity detector (TCD), which detected the carbon oxides, and the other sampled to a flame ionization detector (FID), which detected MA, acetic acid and unreacted *n*-butane.

The reactor comprised of a 9 mm inner diameter quartz tube of 30 cm length. The catalyst was packed undiluted into the reactor. A carborundum packing was employed before the catalyst bed to preheat the feedgas before it reached the catalyst in the reactor.

The precursor, calcined and used catalysts were characterized, the results of which appear in Table 1. Bulk analyses of the catalysts were performed via inductively coupled plasma-atomic emission spectroscopy (ICP-AES) to determine the promoter loading and P:V ratio (Table 1). Energy dispersive X-ray analysis (EDX) was a surface study of the catalyst to determine the promoter loading and the P:V ratio (Table 1). The average vanadium oxidation state (AV) was determined titrimetrically (Table 1). The Brenauer-Emmet-Teller (BET) surface area determination gives an indication of the different surface areas of the varying promoter loaded catalysts (Table 1).

The X-ray diffractograms of the catalyst precursors indicated the presence of two species, viz. (VO)<sub>2</sub>H<sub>4</sub>P<sub>2</sub>O<sub>9</sub> and VO(HPO<sub>4</sub>)·1/2H<sub>2</sub>O. (VO)<sub>2</sub>H<sub>4</sub>P<sub>2</sub>O<sub>9</sub> and VO(HPO<sub>4</sub>)·1/2H<sub>2</sub>O also gave IR signals in the 900–1300 cm<sup>-1</sup> region of the IR spectra of the catalyst precursors. The calcined catalyst was amorphous in nature and its diffraction pattern could not be recorded. The diffraction pattern of a used 2.3% cobalt-loaded catalyst, labelled VPO-3u was however recorded due to the crystalline nature of the catalyst after reaction on stream in the reactor. There was thus a transition of the catalyst from an amorphous state (calcined catalyst) to a crystalline state (used catalyst). The X-ray diffractogram of the used VPO catalyst indicated an orthorhombic structure of the catalyst, which was characteristic of the (VO)<sub>2</sub>P<sub>2</sub>O<sub>7</sub> phase, which is also proposed as the catalytically active phase [4].

Attenuated total reflectance (ATR), which is an infrared examination of the surface of the catalysts, was performed on the catalysts. A peak around 3400 cm<sup>-1</sup>, which appeared in the normal FT-IR of the precursor, calcined and used catalysts did not appear in the calcined and used catalyst ATR spectra. Normal IR spectra are obtained when the IR beam passes through the sample for a bulk analysis. This peak was attributed to the presence of the alcohol (benzyl alcohol and *iso*-butanol) used in the synthesis. This indicated that the alcohol was absent on the surface of the calcined catalyst but trapped in the lattice. The presence of the trapped alcohol was confirmed, when the catalysts were digested in aqua regia in a microwave digester to give an orange residue. EDX analysis of the orange residue showed the presence of carbon and oxygen, which was attributed to the alcohols used in the synthesis. No P or V was present in the orange residue.

The same types of bands were present in both the FT-IR and ATR spectra. This showed that the anions present on the surface of the catalysts, revealed by the ATR study results, were also present in the bulk of the catalyst shown by the FT-IR study results. The used catalysts showed a single strong sharp band in the region of 940 cm<sup>-1</sup> in the ATR spectra compared to the broad band seen in FT-IR spectra of these used catalysts. The surface of the catalyst contained the crystalline (VO)<sub>2</sub>P<sub>2</sub>O<sub>7</sub> phase as revealed by the XRD spectrum of a used catalyst. This presence of a single distinct crystalline phase is thus believed to be responsible for this sharp band in the ATR study.

SEM images of the catalyst precursors (p), calcined catalysts (c) and used catalysts (u) were recorded. The SEM

Table 1  
Characterisation data of VPO catalysts

Label	ICP-AES results		EDX results		AV	BET area (m <sup>2</sup> g <sup>-1</sup> )
	% Co:V (molar)	P:V (molar)	% Co:V (molar)	P:V (molar)		
VPO-1	0.0	1.10	0.0	0.7–0.8	4.0–4.4	14.83
VPO-2	1.2	1.05	1.2	0.7–0.8	4.0–4.4	16.87
VPO-3	2.3	1.05	2.4	0.7–0.8	4.0–4.4	22.93
VPO-4	4.3	1.03	4.2	0.7–0.8	4.0–4.4	13.22

Table 2  
Data from testing a 2.3% cobalt-loaded catalyst at varying temperature and flowrate

	Temperature (°C) (Flowrate (ml min <sup>-1</sup> ))					
	400 (80)	400 (60)	400 (40)	300 (120)	300 (80)	300 (40)
GHSV/ ml g <sup>-1</sup> h <sup>-1</sup>	4800	3600	2400	7200	4800	2400
% Conversion <i>n</i> -butane	100	100	100	96	73	64
% Yield MA	18	0	0	33	23	15
% Selectivity MA	18	0	0	34	32	23

images of the catalyst precursors and calcined catalysts revealed a plate-like morphology (Figs. 1–3) and thus deviated from the ideal rosette-shape platelets of typical VPO catalysts [5]. VPO-3(p) (Fig. 2) showed a more agglomerated platelet arrangement compared to VPO-1(p) (Fig. 1). The cobalt-doped catalyst (VPO-3(p)) thus underwent a change in morphology compared to the undoped catalyst (VPO-1(p)). The platelets on the surface of VPO-1(p) are larger than those on VPO-3(p). An increase in P:V ratio is known to increase the platelet size [6]. The P:V ratio of VPO-1(p) was slightly greater than those of the other catalysts as seen from ICP-AES results (Table 3). Larger platelets formed as a result of calcining VPO-3(p) (Fig. 2) to yield VPO-3(c) (Fig. 3). The SEM images of the used catalysts VPO-1(u) through to VPO-3(u) were similar and showed signs of disintegration on the surface (Figs. 4–6), however, the SEM image of VPO-4(u) (Fig. 6) differed in that pitting occurred on a smoother surface. The plate-like morphology on the surface of all used catalysts was lost (Figs. 4–6).

### 3. Results

The 2.3% cobalt-promoted catalyst (VPO-3) was tested at 300 and 400 °C, the latter being a typical operating temperature for VPO catalysts (Table 2). The molar carbon mass balance was between 95 and 105% for all catalytic runs. It was clear from the results obtained (Table 2) that higher GHSVs (feedgas flowrate (ml h<sup>-1</sup>)/mass of catalyst (g)) and lower temperatures generally favoured higher yields of MA. The other products obtained during testing were

Table 3  
Residence times of *n*-butane feedgas in the reactor

Catalyst	Reaction conditions		Residence time (s)
	Temperature (°C)	Flowrate (ml min <sup>-1</sup> )	
VPO-1	Varying	120	1.00
VPO-2	Varying	120	1.31
VPO-3	Varying	120	1.21
VPO-4	Varying	120	0.97

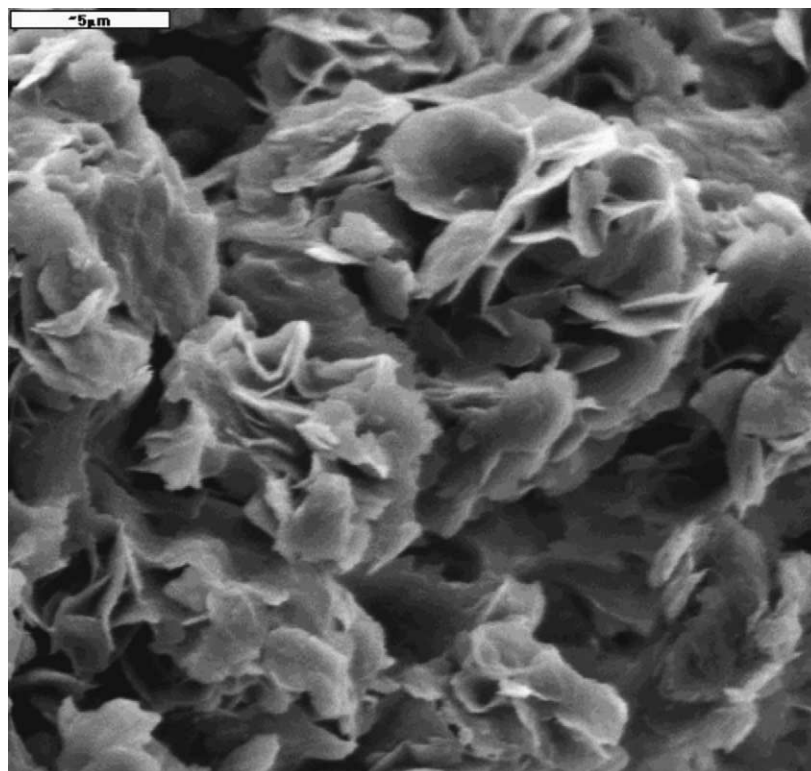


Fig. 1. SEM of VPO-1(p).

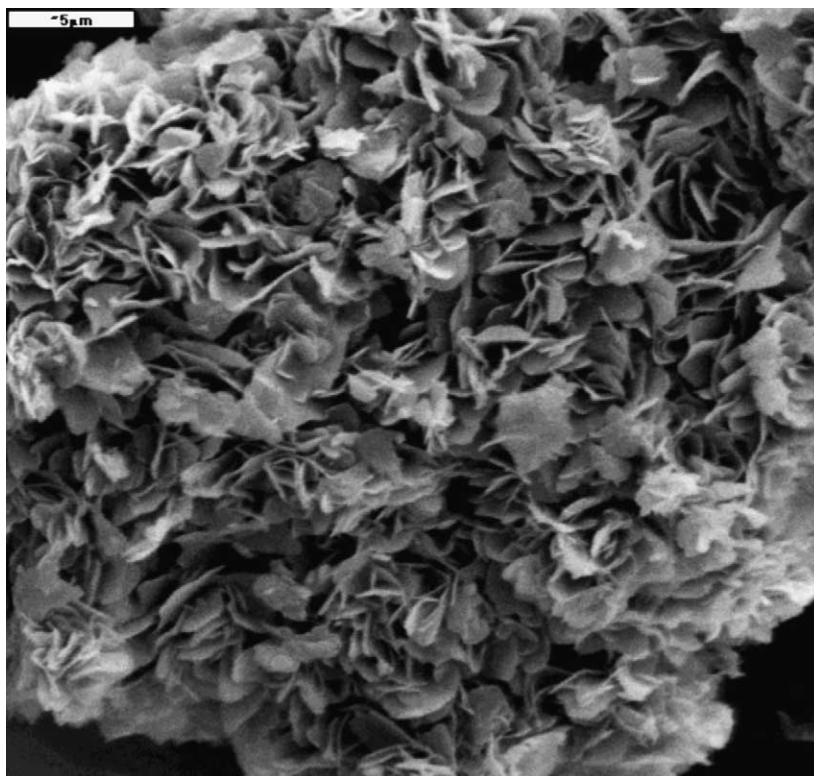


Fig. 2. SEM of VPO-3(p).

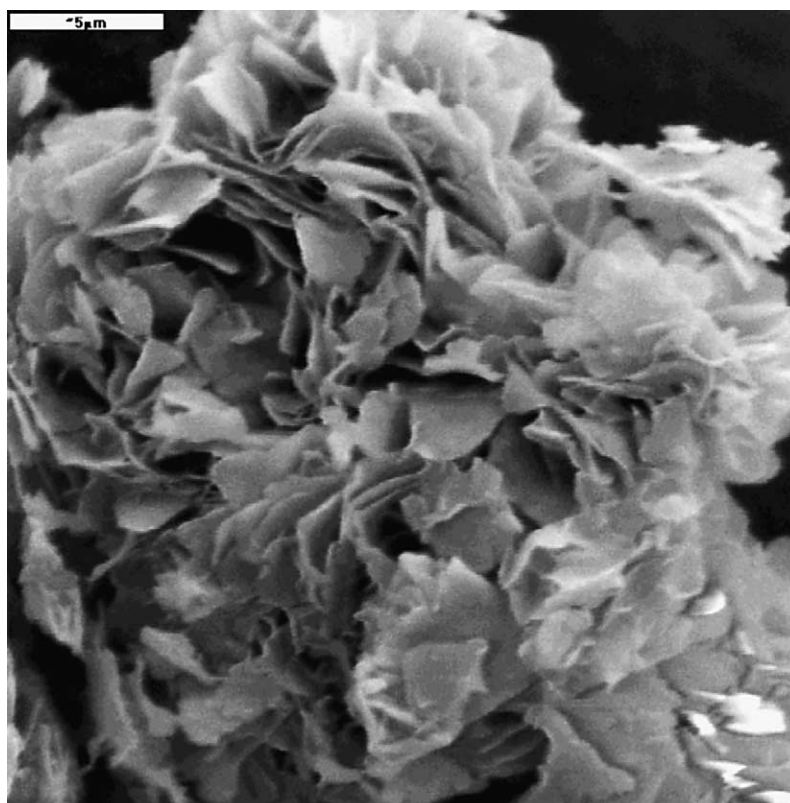


Fig. 3. SEM of VPO-3(c).

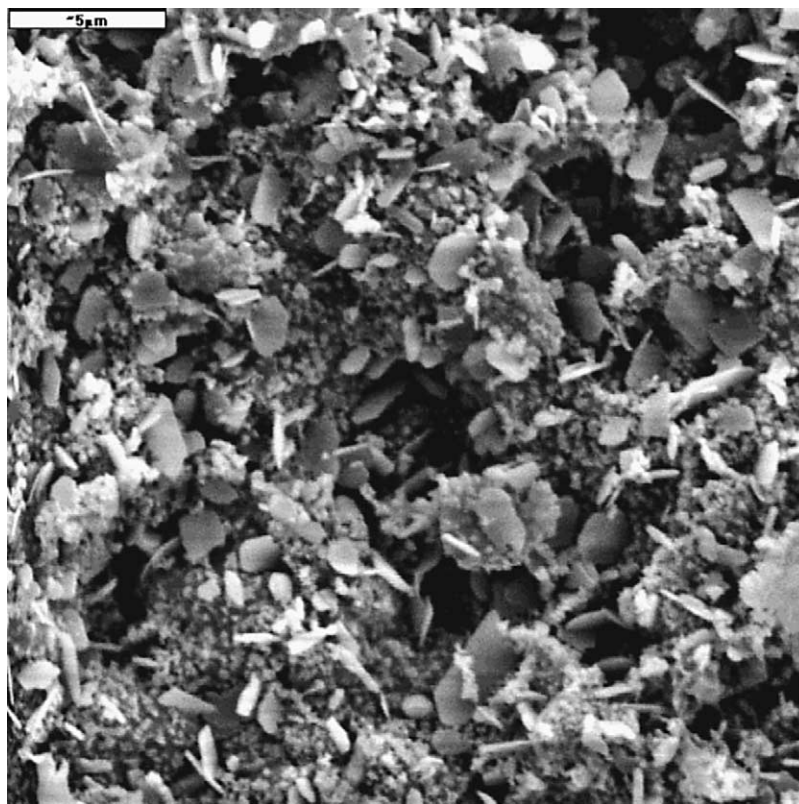


Fig. 4. SEM of VPO-1(u).

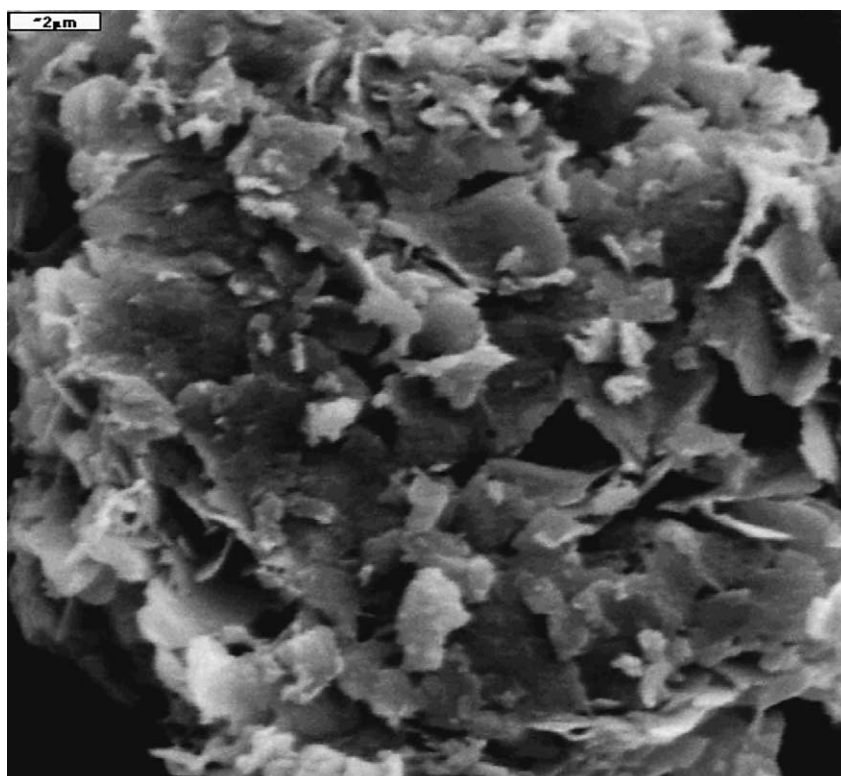


Fig. 5. SEM of VPO-3(u).



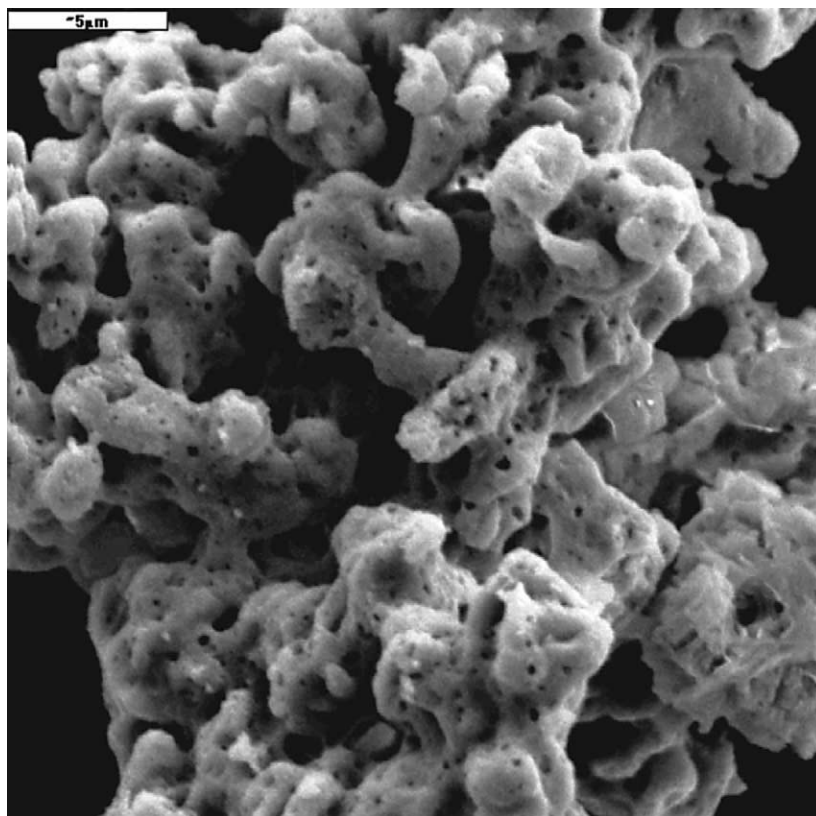


Fig. 6. SEM of VPO-4(u).

carbon monoxide, carbon dioxide and a negligible quantity of acetic acid.

As expected, the conversion of *n*-butane decreased with decreasing temperature. The conversion of *n*-butane was 100% at a constant temperature of 400 °C and varying GHSV's. Carbon oxides were the only products at GHSV's of

2400 and 3600 ml g<sup>-1</sup> h<sup>-1</sup>. MA production at 400 °C was favoured at higher GHSV's. The conversion of butane and the selectivity towards MA increased with increasing GHSV's at a constant operating temperature of 300 °C. It was shown experimentally that the carbon oxide production decreased with increasing GHSV's (Table 2).

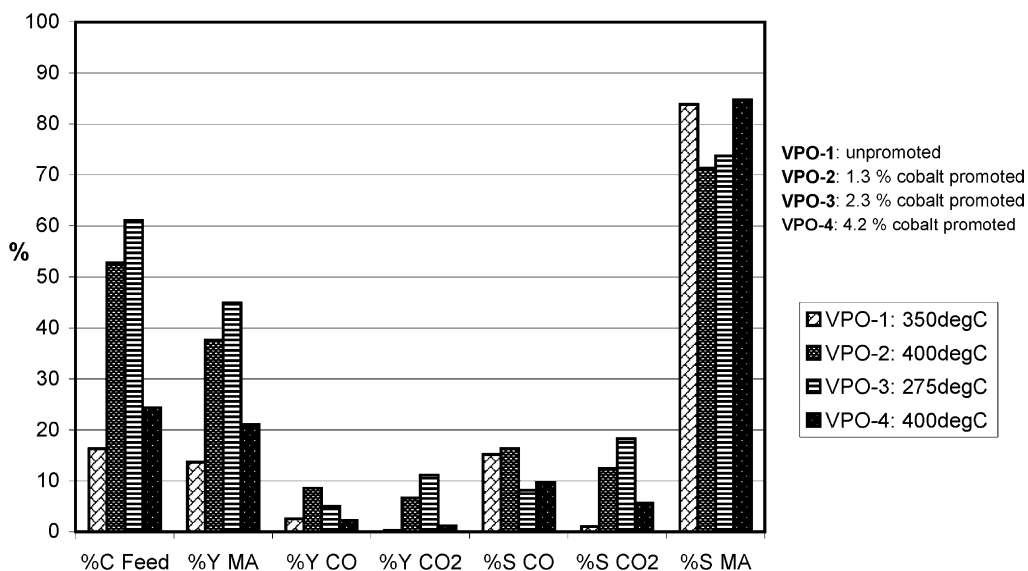


Fig. 7. Composite graph of yield (Y) and selectivity (S) of products and conversion (C) of *n*-butane feedgas, indicating operating temperatures for maximum yields of MA obtained from the four catalysts tested at a constant GHSV of 7200 ml g<sup>-1</sup> h<sup>-1</sup>.

The maximum obtainable feedgas flowrate was  $120 \text{ ml min}^{-1}$  due to reactor constraints and catalyst packing for approximately 1 g of catalyst packed. When the above catalyst was tested at a constant temperature of  $275^\circ\text{C}$  and varying GHSVs greater than  $7200 \text{ ml g}^{-1} \text{ h}^{-1}$ , which was achieved by packing a smaller mass of catalyst, it was established that almost constant yields and selectivity towards MA were obtained.

A flowrate of  $120 \text{ ml min}^{-1}$  was used for systematic testing of the four different promoted catalysts synthesized. This is elaborated on in the discussion. Table 3 shows the feedgas residence times for the four different promoted catalysts. There is a variation in the residence times due to the different volumes of the catalysts packed in the reactor due to varying surface areas (Table 1). One gram of catalyst was used in the testing.

The catalysts were tested between  $200$  and  $500^\circ\text{C}$ . Outside of this range no MA was produced. The selectivity towards MA increases with decreasing temperature, however, it was noted that there was a decrease in *n*-butane conversion with a decrease in temperature for all catalysts tested, as is usual [7]. For each catalyst there exists a maximum yield of MA within the temperature range  $200$ – $500^\circ\text{C}$ . These maximum yields of MA obtained for the different promoted catalysts along with the corresponding feedgas conversions and selectivities and yields of other products are shown in Fig. 7. VPO-1 performed optimally at  $350^\circ\text{C}$  to yield 14% MA with a 17% conversion of *n*-butane (Fig. 7). VPO-2 performed optimally at  $400^\circ\text{C}$  to yield 37% MA with a 53% conversion of *n*-butane (Fig. 7). A low conversion of *n*-butane was expected at a low temperature. However, VPO-3 revealed a MA yield of 45% with a 61% conversion of *n*-butane at  $275^\circ\text{C}$  (Fig. 7). VPO-4 gave a MA yield of 21% with a 24% conversion of *n*-butane at  $400^\circ\text{C}$  (Fig. 7). There thus appears to be an optimum cobalt

promoter loading, which is 2.3 mol% Co versus V. Yields of CO were below 10% for all catalysts under optimal conditions and the  $\text{CO}_2$  yields were below 11% (Fig. 7). Selectivities towards MA higher than 73% were obtained under different conditions. However, these selectivities were obtained at lower conversions of *n*-butane.

The relationship between conversion of *n*-butane and selectivity towards MA for all catalysts tested was examined. A graph of % selectivity towards MA versus % conversion of *n*-butane for the four different promoter-loaded catalysts generally showed a trend of increasing % selectivity towards MA with a decreasing conversion of *n*-butane (Fig. 8). The operating temperature increases on moving from left to right in Fig. 8 and the range was between  $200$  and  $450^\circ\text{C}$ . VPO-3 showed a gradual decrease in % selectivity towards MA with an increase in % *n*-butane conversion. It was only on approaching 100% conversion of *n*-butane that the selectivity fell. VPO-2 followed a similar trend to VPO-3, however, the % selectivities towards MA were lower. VPO-4 showed a steep drop in selectivity towards MA between a conversion of *n*-butane of 30% and 40%. The 2.3% cobalt-loaded catalyst (VPO-3) maintained the highest selectivity towards MA throughout the *n*-butane conversion range, which only dropped rapidly at *n*-butane conversion greater than 95%. Below a butane conversion of 20% in Fig. 8 the selectivity towards MA was erratic due to competing carbon oxide production and the MA yields were below 10%. The catalyst gave greater yields of MA at conversions greater than 20%. An examination of the relationship between the selectivity towards MA and temperature for all four catalysts tested, viz. VPO-1 through to VPO-4, revealed that the selectivity towards MA peaked for VPO-1 and VPO-2 at  $350$  and  $400^\circ\text{C}$  respectively (Fig. 7), which corresponded to the maximum yields of MA obtained for these catalysts. VPO-3 gave progressively

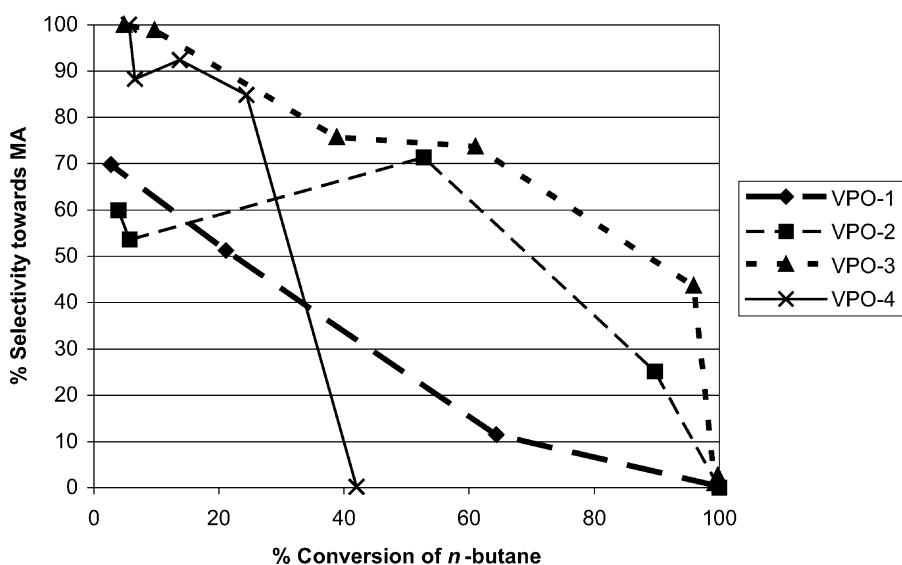


Fig. 8. % Selectivity towards MA vs. % conversion of *n*-butane for four different promoted catalysts, VPO-1 through to VPO-4 at a constant GHSV of  $7200 \text{ ml g}^{-1} \text{ h}^{-1}$ .

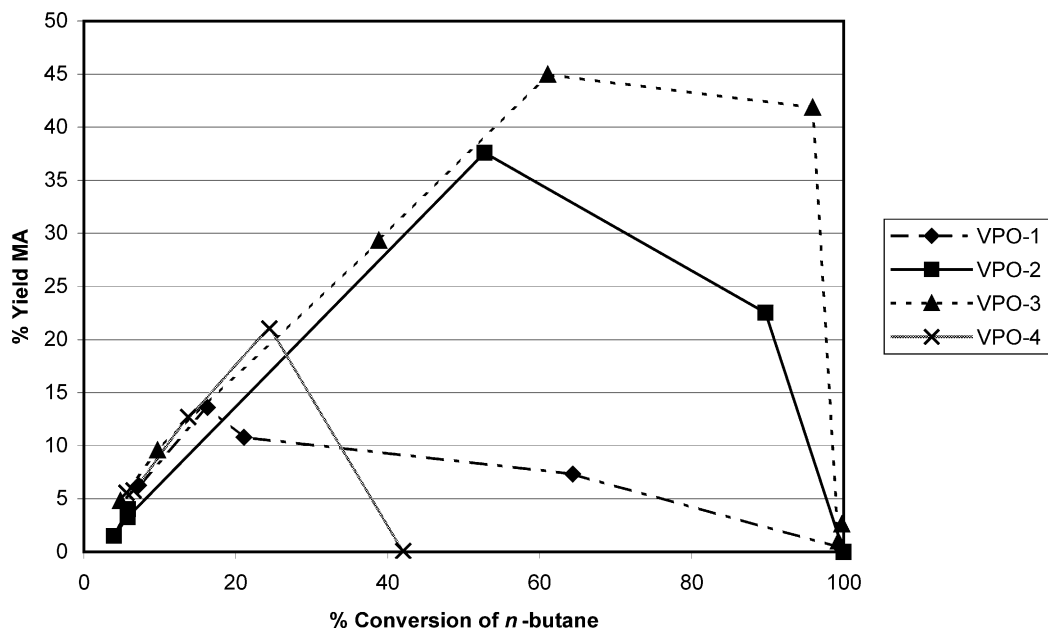


Fig. 9. % Yield MA vs. % conversion of *n*-butane for four different promoted catalysts, VPO-1 through to VPO-4.

increasing selectivity towards MA without peaking with decreasing operating temperature (Fig. 8). VPO-4 (Fig. 8) also showed no distinct peak.

The relationship between yield and conversion is shown in Fig. 9. The MA yields peak at different conversions of *n*-butane for the different catalysts. Catalyst VPO-3 had the highest yield of 45% at the highest conversion of 61% from all the catalysts tested.

#### 4. Discussion

High gas hourly space velocities (GHSV's) and low temperatures favoured MA production. The reason could be attributed to the feedgas having a low residence time in the reactor at higher GHSV's, thus reducing the probability of over-oxidation of the product. Lower temperatures also favour higher selectivity as the carbon oxide by-products are only favoured at higher temperatures [8]. A constant flow-rate of 120 ml min<sup>-1</sup> was maintained for all catalyst testing.

It can also be seen from the results in Table 2 that MA was produced at 80 ml min<sup>-1</sup> and not at lower flowrates, when the catalyst was tested at 400 °C. It is thus possible that the MA was further oxidized at lower flowrates.

It is usual for *n*-butane conversion to increase with temperature. When comparing the catalysts at an operating temperature of 275 °C, VPO-3 gave the highest conversion of 61%. The other catalysts gave conversions less than 10% at this operating temperature. The addition of cobalt thus affects the catalytic performance of VPO catalysts. Zazhigalov et al. [9] showed in a study that adsorption of ammonia onto the catalyst increased with increasing cobalt content, between a promoter loading range of 0–0.20 mol%, which indicated increased acidity. Introduction of small

amounts of cobalt into the VPO catalyst mainly caused the appearance of weak acid sites, whereas the number of strong acid sites was raised to a lesser extent. The acidity of the catalyst influences the selectivity of the catalyst. A slightly acidic catalyst reduces the time the acidic MA product spends on the catalyst, thus reducing the chance of further oxidation of the product [10]. The cobalt promoter loading also resulted in a change in BET surface area of the catalyst as seen from the results in Table 1.

The highest yield of MA was obtained over VPO-3 at a temperature of 275 °C. At 275 °C, this catalyst also gave the highest conversion of butane of the four catalysts tested under optimized conditions. This suggests that the optimum cobalt promoter loading on the catalyst was 2.3% (Table 1).

The best performing catalyst had the highest surface area and thus the effect of surface area was examined under the optimum operating conditions (Fig. 10) for each catalyst.

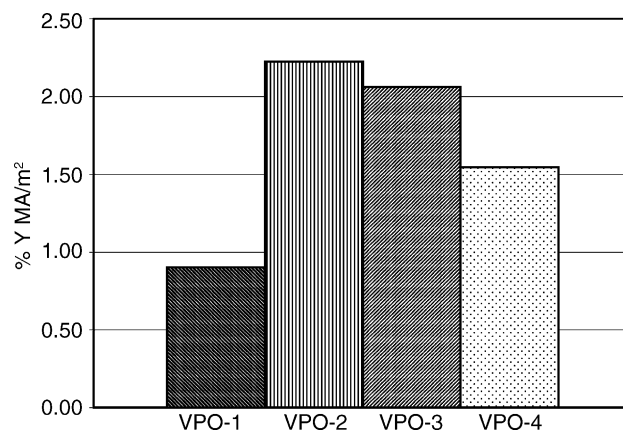


Fig. 10. Graph of specific % yield MA for optimum catalytic conditions for catalysts VPO-1 through to VPO-4.



Fig. 10 indicates that the specific yield of MA (i.e. the yield MA/total surface area of catalyst in the reactor) was different for the different catalysts at varying optimum operating temperatures. The specific conversions and specific selectivity for the four catalysts examined under optimum operating conditions were different as well. It was thus concluded that the varying surface areas of the catalyst could not exclusively explain the differences in yield, selectivity and conversion under optimum conditions.

VPO-3 maintained the highest selectivity towards MA of the four catalysts tested shown in Fig. 8. This was due to the cooler operating temperatures over which this catalyst converted *n*-butane to MA. The following selectivity towards MA were obtained at a constant conversion of 40% (Fig. 8) when comparing the four catalysts tested: VPO-1 (35%), VPO-2 (66%), VPO-3 (76%) and VPO-4 (10%).

The highest yield of MA obtained was 45% at a conversion of 61% for VPO-3. The following selectivity towards MA was obtained at a constant conversion of 61% (Fig. 8), when comparing the four catalysts tested: VPO-1 (14%), VPO-2 (58%), VPO-3 (74%) and VPO-4 (0%). VPO-3 gave the highest selectivity towards MA, when comparing the four catalysts tested at a constant conversion of 61%. The relationship between yield of MA and conversion of *n*-butane is shown in Fig. 9. The other catalysts produced lower yields of MA at a 61% conversion of *n*-butane.

The cobalt dopant modified the surface structure of VPO-3(p) as seen by comparing the SEM image of the unpromoted catalyst (Fig. 1) and the promoted catalyst VPO-3(p) (Fig. 2). The more agglomerated plate-like arrangement of VPO-3p could be part of the reason for the improved performance of the catalyst.

SEM images of the used catalysts (Figs. 4–6) showed some disintegration on the surface of the catalysts. This maybe due to the constant oxidation and reduction taking place on the surface of the catalyst. The performance of the catalysts, however, did not change over the times they were tested (approximately 200 h).

XRD spectra indicated the presence of the active catalytic phase,  $(VO)_2P_2O_7$ , in the used catalyst, which was formed from the  $VO(HPO_4) \cdot 1/2H_2O$  precursor. XRD spectra also showed the modification of the catalyst structure with the addition of cobalt. The addition of cobalt resulted in a less-crystalline catalyst structure as indicated by the decrease in intensities of the spectral lines from unpromoted to promoted catalyst. Defects in catalyst structure result in a less-crystalline catalyst, which in turn improves selectivity towards MA [11].

ATR analysis of the catalyst surface showed the absence of the alcohol on calcination of the catalyst precursor. However, the FT-IR spectrum of the calcined and used catalysts, using the KBr pellet method of analysis which was a bulk catalyst study, still showed the presence of the alcohol. This indicated that the alcohol was trapped in the lattice of the catalyst.

ATR studies of the catalysts confirmed that the catalytically active crystalline phase  $(VO)_2P_2O_7$  is prominent on the surface of the catalyst as indicated by a single distinct peak at  $2\theta = 35.5^\circ$ . A broad band in the FT-IR spectrum at  $\sim 3400\text{ cm}^{-1}$  is probably due to the alcohol present in the lattice of the catalyst, which may reduce crystallinity.

The AV was around 4.3 on average for all catalysts after conditioning and testing the catalysts in the reactor. This indicated an oxidation state switching between +4 and +5 in the oxidation of *n*-butane to MA.

A slight excess of phosphorous in the catalyst, i.e. a molar P:V ratio greater than 1 is necessary to stabilise the active phase [12]. The molar P:V ratios of the catalysts from the precursor through to the calcined and used catalysts, remained constant at around 1.1 in the bulk of the catalyst and 0.80 on the surface of the catalyst (Table 1). Cobalt maintained the bulk P:V ratio around 1.1 during testing of the catalyst (up to 2000 h) with no loss of phosphorous observed, thus confirming that Co prevents loss of phosphorous [3]. It is generally accepted that inclusion of phosphorous above the stoichiometric amount stabilises the  $V^{4+}$  valence state, and limits its oxidation [13].  $V^{4+}$  at the surface of the pyrophosphate is proposed to activate molecular oxygen, while the surface layer can be oxidised to a certain extent to  $V^{5+}$ , which provides the capacity to oxidise adsorbed hydrocarbons. By maintaining most of the vanadium in the +4 oxidation state, the probability of over-oxidation of MA is reduced and this results in a high selectivity towards MA.

We conclude that the method of preparation and calcination is crucial in the preparation of VPO-type oxidation catalysts. This has permitted the preparation of a catalyst that is functional at lower temperatures than conventional catalysts [14–17], giving the benefit of the higher selectivity towards MA at lower temperatures and conversions [18]. There is clearly an optimum amount of promoter, which is around 2.3%. This promoter increases the surface area of the catalyst and also modifies the catalyst surface.

Most industrial catalysts are capable of a conversion of *n*-butane in the region of 70–90 mol%. Their yields of MA are in the region of 55–65 mol%. Selectivity approach 90 mol% with lower conversions than those mentioned above. The selectivities are, however, generally around 60–70 mol% on average.

The optimum catalyst obtained in this study gave a yield of 45 mol%. The conversion of *n*-butane was 62% with corresponding % selectivity towards MA of 73%. The optimally promoter loaded catalyst VPO-3 gave the highest yield MA at the highest conversion of *n*-butane from all the catalysts tested in this study.

The yield of MA is lower than that obtained industrially. However, the optimal catalyst achieved the 45% yield at temperature more than 100 °C cooler than industrially operated catalysts.

## Acknowledgements

We thank Klaus Möller (UCT) and Basil Chasoullas (Wits) for invaluable advice on reactor design and THRIP for financial support. We also thank Fiona Graham for the electron microscopy.

## References

- [1] G. Centi, F. Cavani, F. Trifirò, *Selective Oxidation by Heterogenous Catalysis*, Kluwer academic/Plenum publishers, 2001, p. 144.
- [2] F. Ben Abdelouahab, R. Olier, M. Ziyad, J.C. Volta, *J. Catal.* 157 (1995) 687.
- [3] F. Trifirò, *Catal. Today* 16 (1993) 91.
- [4] M.R. Thompson, A.C. Hess, J.B. Nicholas, J.C. White, J. Anchell, J.R. Ebner, *New Developments in Selective Oxidation II* (1994) 167.
- [5] R.W. Wenig, G.L. Schrader, *J. Phys. Chem.* 90 (1986) 6480.
- [6] W. Cheng, *Appl. Catal. A: Gen.* 147 (1996) 55–67.
- [7] G. Centi, F. Trifirò, *Cat. Today* 3 (1988) 155.
- [8] G. Busca, G. Centi, F. Trifiro, *Appl. Catal.* 25 (1986) 268.
- [9] V.A. Zazhigalov, J. Haber, J. Stoch, A.I. Pyatnitskaya, G.A. Komashko, V.M. Belousov, *Appl. Catal. A: Gen.* 96 (1993) 135.
- [10] G. Centi, F. Trifirò, *Appl. Catal.* 12 (1984) 1.
- [11] F. Cavani, A. Colombo, F. Trifirò, M.T. Sananes-Schulz, J.C. Volta, G.J. Hutchings, *Catal. Lett.* 43 (1997) 241–247.
- [12] B.K. Hodnett, B. Delmon, *Ind. Eng. Chem. Fundam.* 23 (1984) 465.
- [13] B.K. Hodnett, *Cat. Rev-Sci. Eng.* 27 (3) (1985) 373–424.
- [14] L.M. Cornaglia, C.R. Carrar, J.O. Petunchi, E.A. Lombardo, *Appl. Catal. A: Gen.* 183 (1999) 177–187.
- [15] M.T. Sananes-Schulz, A. Tuel, G.J. Hutchings, J.C. Volta, *J. Catal.* 166 (38) (1997) 392.
- [16] F. Ben-Abdelouahab, R. Olier, M. Ziyad, J.C. Volta, *J. Catal.* 157 (1995) 687–697.
- [17] S. Sajip, J.K. Bartley, A. Burrows, M.T. Sananes-Schulz, A. Tuel, J.C. Volta, C.J. Kiely, G.J. Hutchings, *New J. Chem.* 25 (2001) 125–130.
- [18] L. Cornaglia, S. Irusta, E.A. Lombardo, M.C. Durupty, J.C. Volta, *Catal. Today* 78 (2003) 294.